Supplementary information for:

Pharmacologic inhibition of histone demethylation as a therapy for pediatric brainstem glioma

Rintaro Hashizume[1], Noemi Andor[2], Yuichiro Ihara[2], Robin Lerner[2], Haiyun Gan[3], Xiaoyue Chen[3], Dong Fang[3], Xi Huang[4], Maxwell W. Tom[2], Vy Ngo[5], David Solomon[6,7], Sabine Mueller[2,8,9], Pamela L. Paris[5], Zhiguo Zhang[3], Claudia Petritsch[2], Nalin Gupta[2], Todd A. Waldman[7] and C. David James[1]

[1]Department of Neurological Surgery, Feinberg School of Medicine, Northwestern University, Chicago, IL, USA
[2]Department of Neurological Surgery, University of California, San Francisco, San Francisco, CA, USA
[3]Department of Biochemistry and Molecular Biology, Mayo Clinic, Rochester, MN, USA
[4]Department of Physiology, University of California, San Francisco, San Francisco, CA, USA
[5]Department of Urology, University of California, San Francisco, San Francisco, CA, USA
[6]Department of Pathology, University of California, San Francisco, San Francisco, CA, USA
[7]Lombardi Comprehensive Cancer Center, Georgetown University School of Medicine, Washington, D.C., USA
[8]Department of Neurology, University of California, San Francisco, San Francisco, CA, USA
[9]Department of Pediatrics, University of California, San Francisco, San Francisco, CA, USA

Corresponding Author:
Rintaro Hashizume, MD, PhD
Department of Neurological Surgery
Feinberg School of Medicine, Northwestern University
300 E Superior Street
Tarry Building 2-709
Chicago, IL 60611
Phone: 312-503-3822
Fax: 312-503-3552
E-mail: rintaro.hashizume@northwestern.edu

Supplementary Table 1

Cell Source	Age/G	Diagnosis	Location	Known Mutation
SF7761	6/F	DIPG	Pons	*H3F3A* K27M
SF8628	3/F	DIPG	Pons	*H3F3A* K27M
SF9012	17/F	GBM	Front-parietal	*PTEN* deletion
SF9402	6/F	GBM	Cerebellum	*EGFR* amplification
SF9427	9/F	GBM	Frontal	None identified
KNS42	16/M	GBM	Front-parietal	*H3F3A* G34V
GBM43	69/M	GBM	Temporal	*TP53* F270C
				CDKN2A null

In addition to the genes indicated above, these tumors were also analyzed and determined to be of wild type sequence for *BRAF, IDH1, HIST1H3B, PTEN*. G, gender; F, female; M, male.

Supplementary Table 1. **Clinical characteristics of patients whose tumors were used to derive the cell lines used in this report.**

Supplementary Figure 1

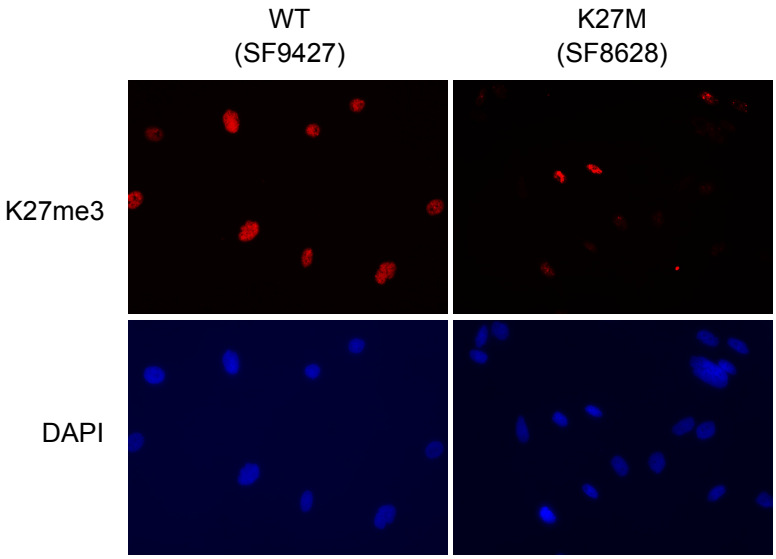

Supplementary Figure 1. Comparison of K27me3 expression in K27 wild-type (SF9427) and K27M mutant (SF8628) glioma cells by fluorescence immunocytochemistry. Results show lesser K27me3-associated fluorescence in K27M cells. DNA staining is by DAPI. WT, wild type.

Supplementary Figure 2

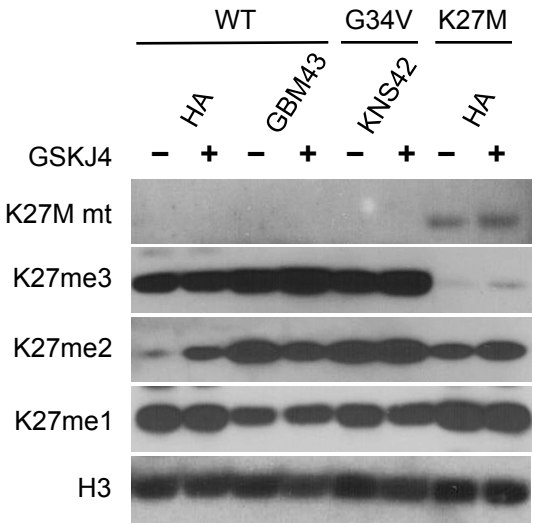

Supplementary Figure 2. GSKJ4 increases K27 methylation in human astrocytes (HAs) with transgene expression of K27M mutation. Results from immunoblot analysis of K27M mt, K27me3, K27me2, K27me1, and total histone H3 in additional K27 wild type and G34V mutant glioma cells, as well as HAs with and without transgene expression of K27M mutation, and treated with or without 6 μM (HA WT, GBM43, KNS42) or 5 μM (HA K27M) GSKJ4 for 72 h.

Supplementary Figure 3

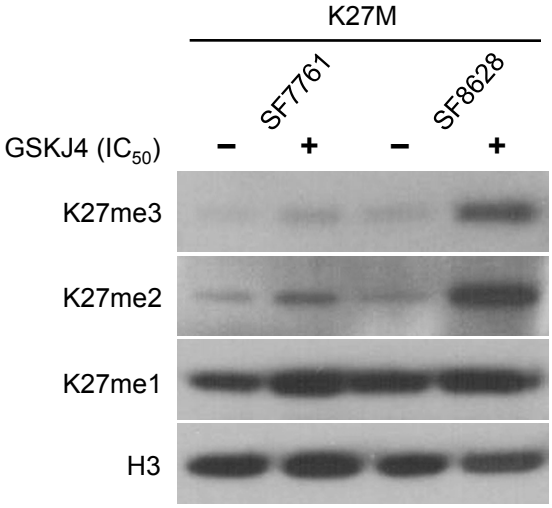

Supplementary Figure 3. IC_{50} concentrations of GSKJ4 increase K27 methylation in K27M glioma cells. Results from immunoblot analysis of K27me3, K27me2, K27me1, and total histone H3 in K27M glioma cells (SF7761 and SF8628) treated with their respective IC_{50} concentrations of GSKJ4 (**Fig. 1d**) for 72 h.

Supplementary Figure 4

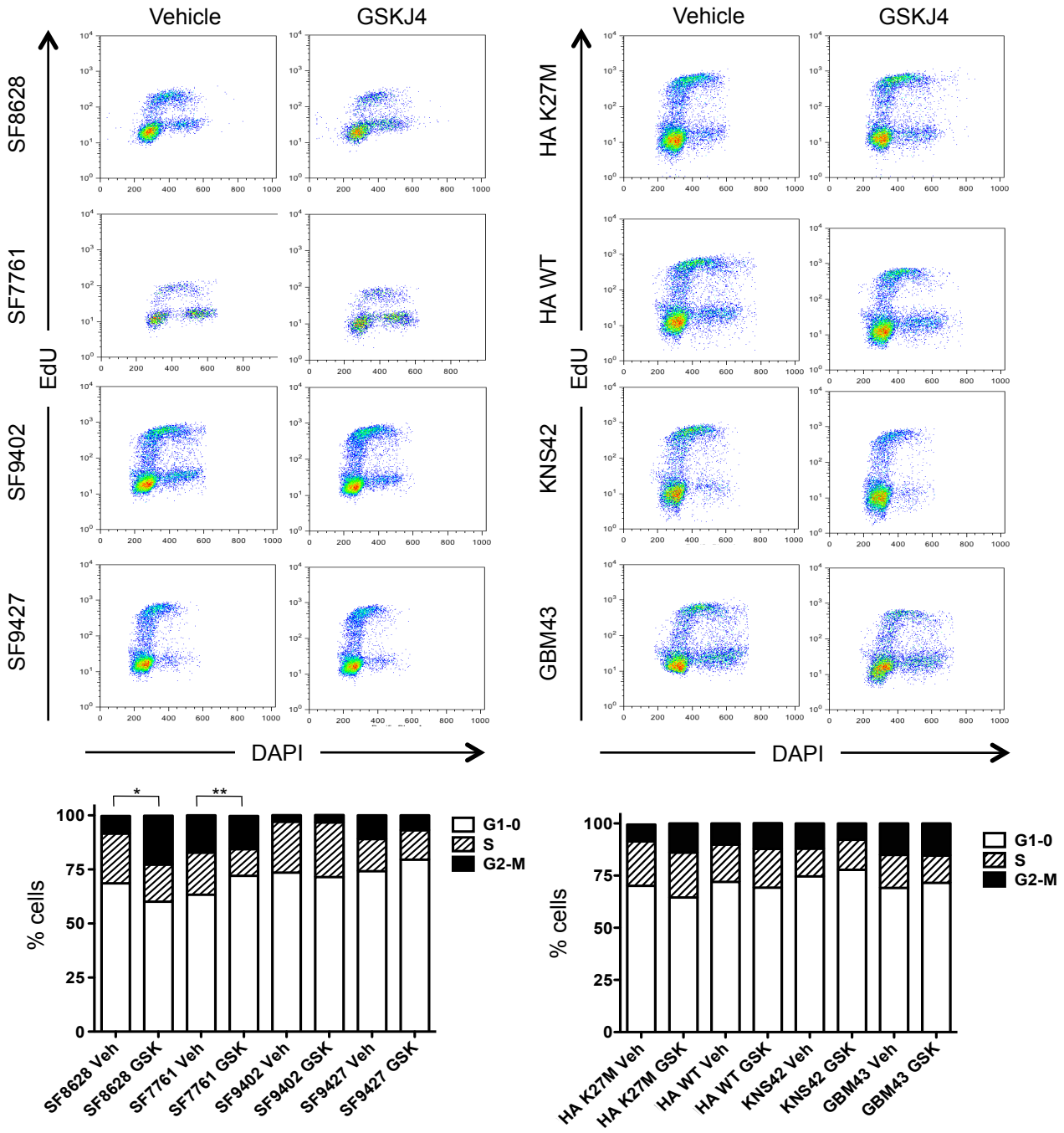

Supplementary Figure 4. Analysis of GSKJ4 effects on cell cycle distributions. Cells were treated with 3 μM GSKJ4 for 72 h, then pulsed with 10 μM EdU for 30 min, then stained with DAPI, then analyzed by flow cytometry. Cell sorting scatter plots for vehicle and GSKJ4 treated cells are shown above, with graphs below showing cell cycle composition for each cell type and each treatment (Unpaired *t*-test values for comparisons between vehicle and GSKJ4 treatment in SF8628 and SF7761 cells, * $P < 0.010$; ** $P < 0.001$).

Supplementary Figure 5

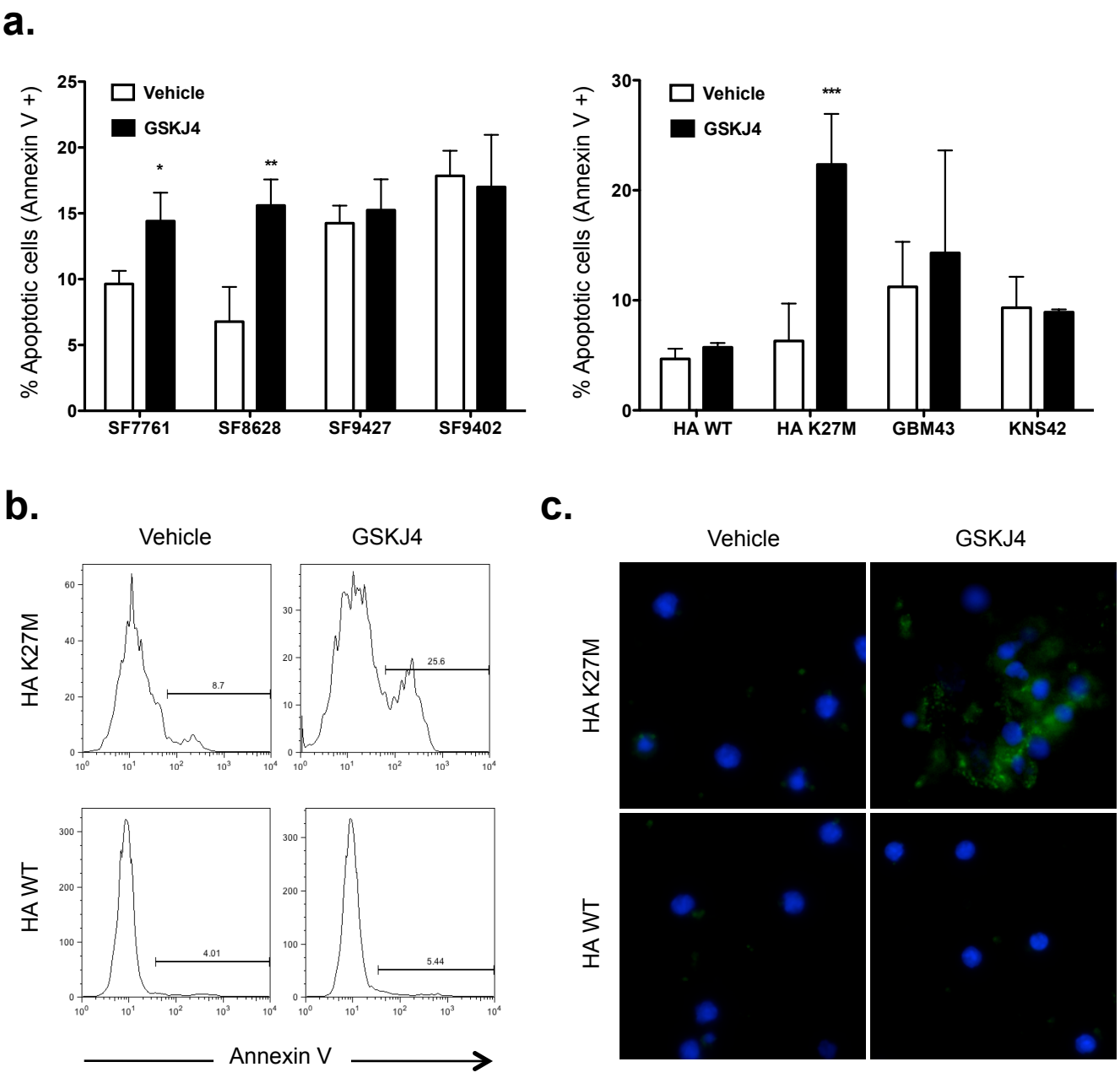

Supplementary Figure 5. Annexin V flow cytometry analysis of GSKJ4 apoptosis effects. Cells were treated with 3 μM GSKJ4 for 72 h, then collected and treated with Alexa Fluor 488 Annexin V, then flow sorted. Annexin V positivity results are shown above for all cell sources and values shown are the average (mean ± SEM) from triplicate samples (2-Way ANOVA with Bonferroni post-test value comparisons between each cell lines, * P = 0.0068; ** P = 0.0010; *** P = 0.0064) (**a**)**,** with examples of annexin V flow sorting profiles (**b**) and annexin V immunocytochemistry (**c**) shown below.

Supplementary Figure 6

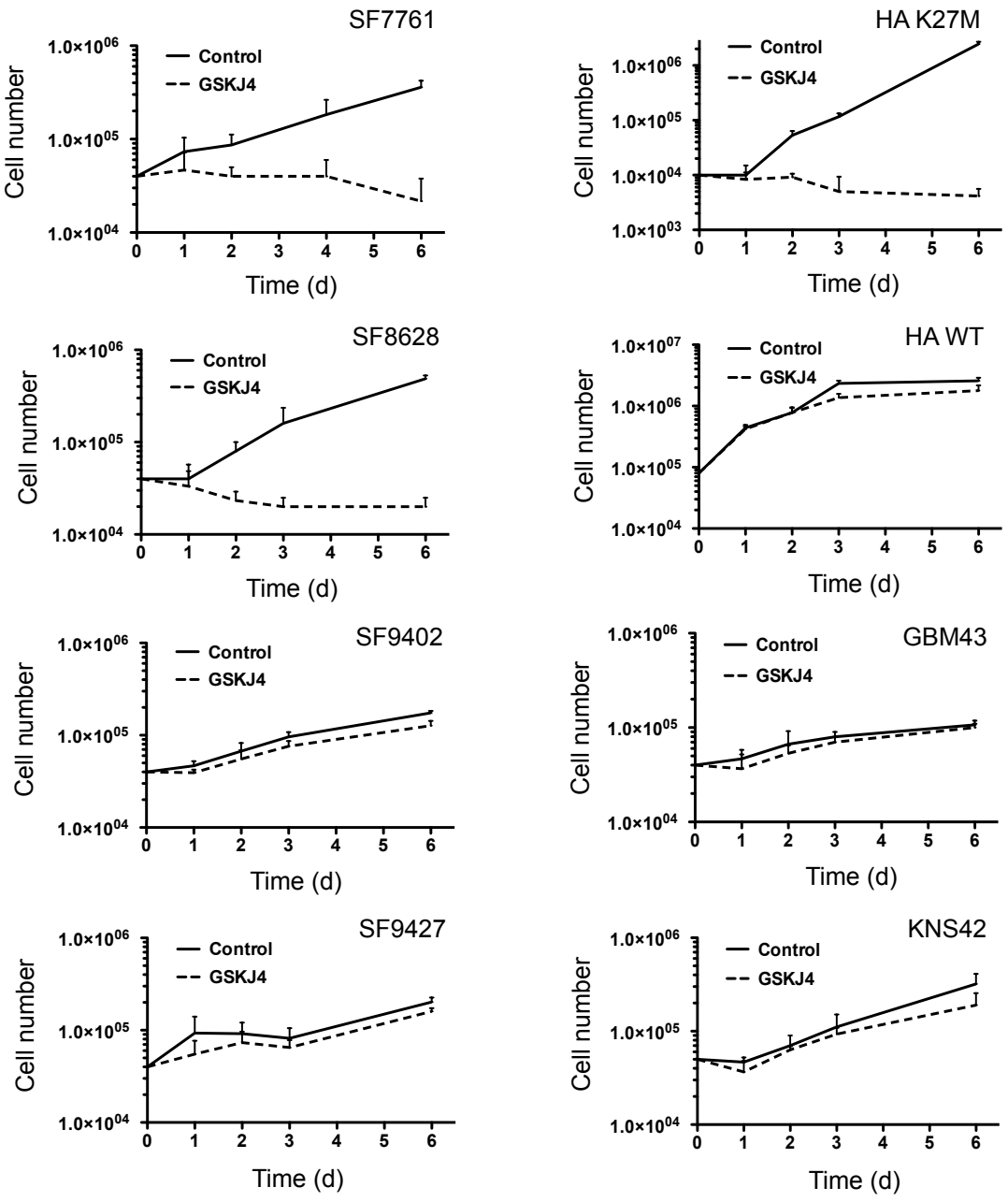

Supplementary Figure 6. Analysis of GSKJ4 effects on cell number. Cells were plated then treated with respective IC_{50} concentrations (**Fig. 1d**) of GSKJ4 or vehicle only (control), then collected and counted following 1–6 d of incubation with inhibitor. Results for each time point are based on triplicate samples. Note that y-axes are in log scale.

Supplementary Figure 7

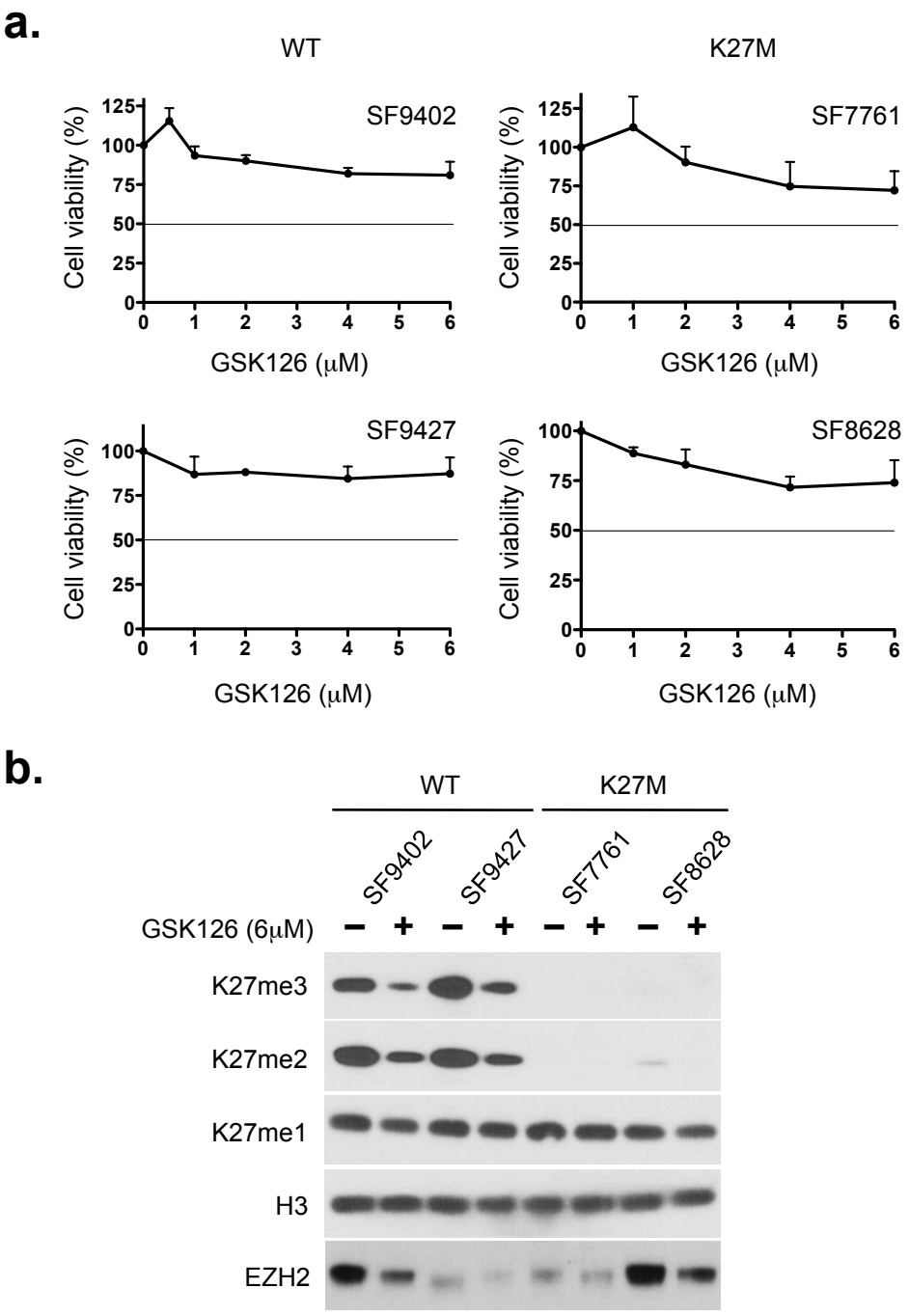

Supplementary Figure 7. Effect of EZH2 inhibitor GSK126 on glioma cell growth and K27 methylation. (**a**) Cell growth plots showing variable, but consistently modest anti-proliferative effect of 72 h incubations with EZH2 inhibitor GSK126 at concentrations of 1–6 μM. Values shown are the average (mean ± SEM) from quadruplicate samples for each incubation condition. (**b**) Immunoblot results showing reductions in K27me3 and K27me2 following 72 h incubation with 6 μM GSK126.

Supplementary Figure 8

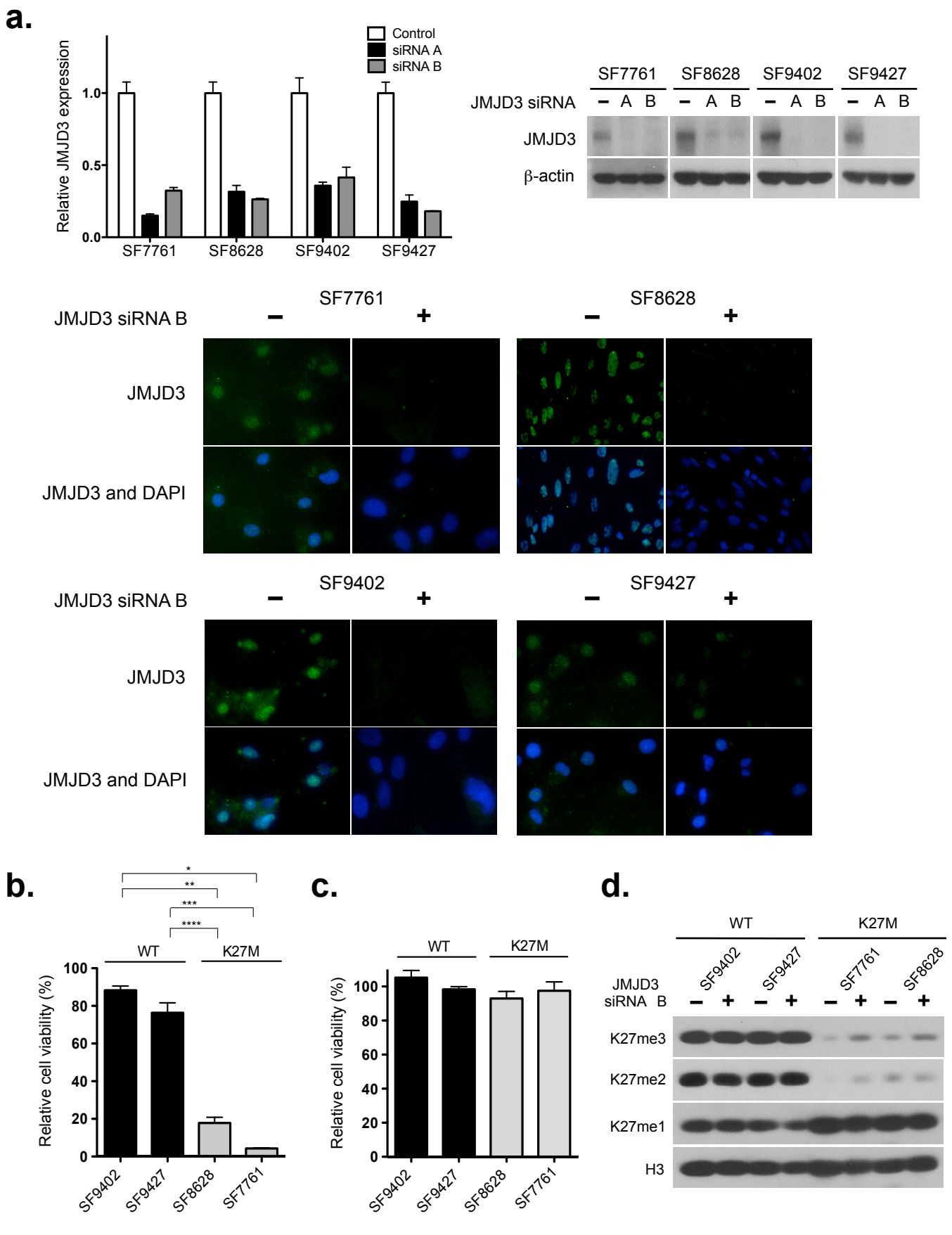

Supplementary Figure 8. Effect of JMJD3 siRNA on glioma cell proliferation and GSKJ4 inhibitor response. (**a**) Indicated cell types were treated with 30 nM JMJD3 siRNA (A, s23109; B, s23110), or scrambled siRNA for 96 h, then examined by quantitative RT-PCR for mRNA expression (upper left) and immunobloting for protein expression (upper right). Values shown are the average fold change (mean ± SEM) from three independent experiments relative to the control, which was given a value of one. Fluorescence immunocytochemistry indicates JMJD3 expression in the cells treated with JMJD3 siRNA B (s23110). (**b**) Cell viability assay results are based on absorbance values of JMJD3 siRNA B (s23110) treated cells relative to corresponding scrambled siRNA treated cells, with each histogram value based on averages from triplicate samples (mean ± SEM). Unpaired *t*-test values for comparisons between cell lines, * $P < 0.0001$; ** $P < 0.0001$; *** $P = 0.0002$; **** $P = 0.0006$. (**c**) Cells treated with siRNAs for 96 h were then treated with IC_{50} concentrations (SF7761 and SF8628) or 6 μM (SF9402 and SF9427) GSKJ4 for 72 h, then analyzed for effect of GSKJ4 treatment on proliferation by cell viability assay. Values shown are based on ratios of GSKJ4 and siRNA treated cells vs. corresponding siRNA only treated cells and the averages from triplicate samples (mean ± SEM). (**d**) Western blot results showing effects of JMJD3 siRNA B (s23110) treatments (+) on expression of K27me3, K27me2, K27me1, and total histone H3.

Supplementary Figure 9

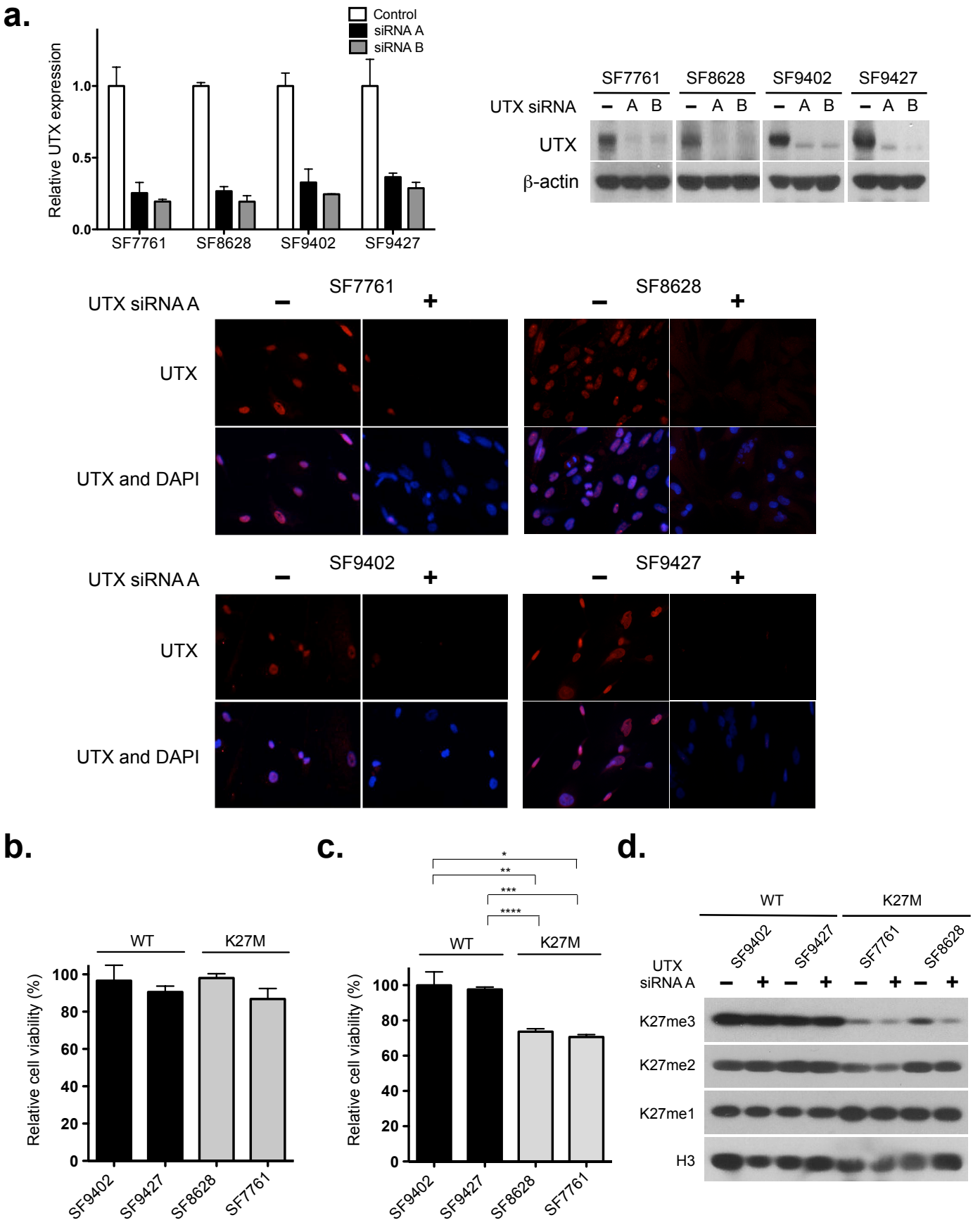

Supplementary Figure 9. Effect of UTX siRNA on glioma cell proliferation and GSKJ4 inhibitor response. (**a**) Indicated cell types were treated with 30 nM UTX (A, s14737; B, s14736), or scrambled siRNA for 96 h, then examined by quantitative RT-PCR for mRNA expression (upper left) and immunoblotting for protein expression (upper right). Values shown are the average fold change (mean ± SEM) from three independent experiments relative to the control, which was given a value of one. Fluorescence immunocytochemistry indicates UTX expression in the cells treated with UTX siRNA A (s14737)**.** (**b**) Cell viability assay results are based on absorbance values of UTX siRNA A (s14737) treated cells relative to corresponding scrambled siRNA treated cells, with each histogram value based on averages from triplicate samples (mean ± SEM). (**c**) Cells treated with siRNAs for 96 h were then treated with IC_{50} concentrations (SF7761 and SF8628) or 6 μM (SF9402 and SF9427) GSKJ4 for 72 h, then analyzed for effect of GSKJ4 treatment on cell proliferation by cell viability assay. Values shown are based on ratios of GSKJ4 and siRNA treated cells vs. corresponding siRNA only treated cells and the averages from triplicate samples (mean ± SEM). Unpaired *t*-test values for comparisons between cell lines, * $P = 0.0195$; ** $P = 0.0281$; *** $P = 0.0001$; **** $P = 0.0004$. (**d**) Western blot results showing effects of UTX siRNA A (s14737) treatments (+) on expression of K27me3, K27me2, K27me1, and total histone H3.

Supplementary Figure 10

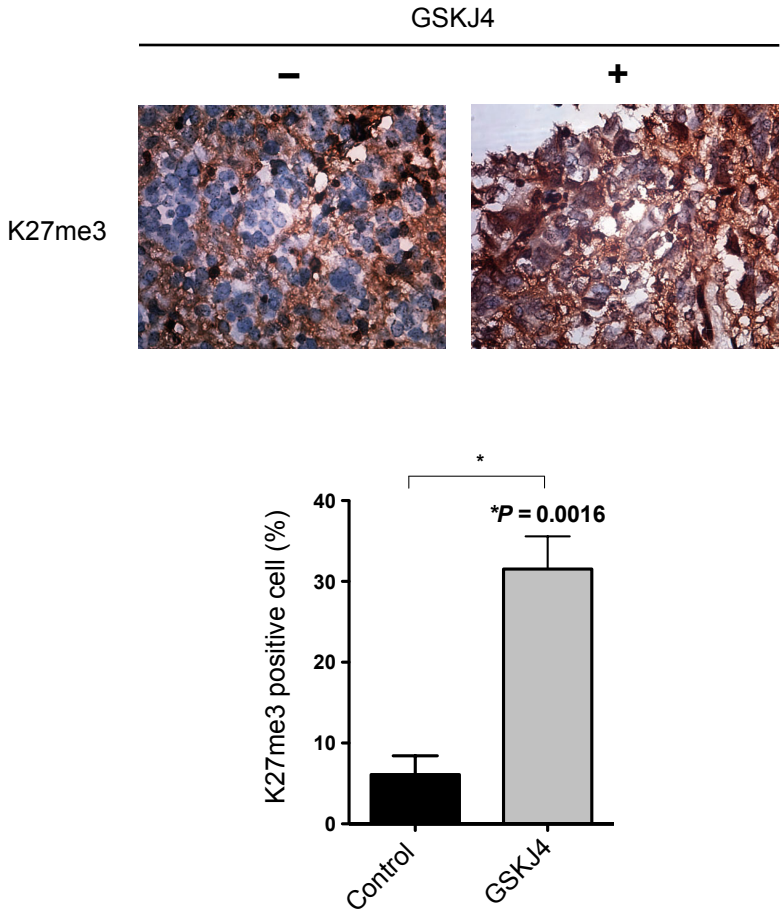

Supplementary Figure 10. Effect of GSKJ4 treatment on K27me3 expression in brainstem SF8628 K27M tumor. Mice with SF8628 brainstem tumor were either treated with vehicle or 100 mg/kg GSKJ4 daily for 10 d, then euthanized, with brains immediately resected for histopathologic processing and subsequent immunohistochemical analysis with K27me3 antibody. Image results show a higher proportion of tumor cells from vehicle (–) treated mice as lacking K27me3 staining, whereas significantly more frequent positive staining is evident in tumor cells from GSKJ4 treated (+) mice. The graph below shows the number of positive cells from vehicle (control) and GSKJ4 treated tumors, with values based on average positive cells counted in four high-powered fields (mean ± SEM). Unpaired *t*-test values for comparisons between control and GSKJ4 treatment, **P* = 0.0016.

Supplementary Table 2

Animal Subject	Brainstem	Hemisphere
M1	3.76	ND
M2	4.58	4.82
M3	9.48	7.46

All entries represent ng/ml GSKJ1. GSKJ4 was not detected (ND) in any specimen.

Supplementary Table 2. **Inhibitor concentrations in mouse brain tissues.**

Supplementary Figure 11

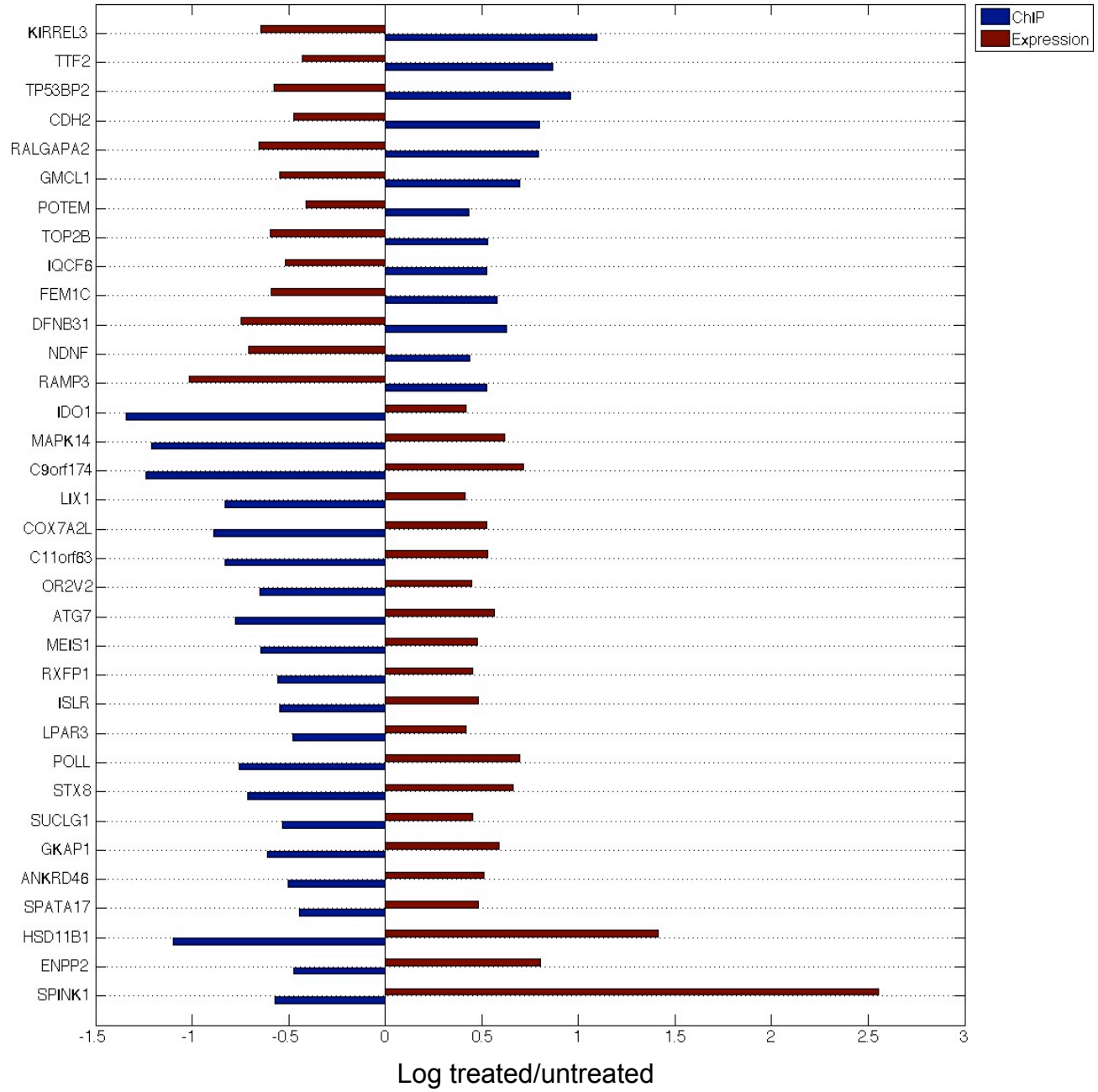

Supplementary Figure 11. Inverse correlation between GSKJ4 associated gene expression and K27me3 immunoprecipitation changes. SF8628 cells were treated with 6 μM GSKJ4 for 24 and 72 h, with K27me3 chromatin immunoprecipitated and examined for gene sequence content. Treated cells were also used for obtaining RNA that was examined for transcriptome effects of treatment. Results show fold change (natural logarithm) in sequence immunoprecipitation and corresponding gene expression changes from treatment.

Supplementary Table 3

	K27me3 ChIP		Gene Expression	
Gene	Log G/V	*P*-value	Log G/V	*P*-value
SPINK1	-0.5725	0.00671	2.55568	0.01426
ENPP2	-0.47296	0.073	0.80505	0.07553
HSD11B1	-1.09766	0.04688	1.41069	0.08904
SPATA17	-0.44512	0.02012	0.48251	0.00695
ANKRD46	-0.50423	0.09296	0.51053	0.0362
GKAP1	-0.609	0.02002	0.59152	0.03415
SUCLG1	-0.53281	0.09058	0.45094	0.07826
STX8	-0.71127	0.08984	0.66405	0.03689
POLL	-0.75434	0.02985	0.69465	0.02214
LPAR3	-0.47976	0.06171	0.41912	0.00898
ISLR	-0.54628	0.04883	0.48236	0.01175
RXFP1	-0.55439	0.08325	0.4525	0.0289
MEIS1	-0.64469	0.07812	0.4766	0.049
ATG7	-0.77838	0.07031	0.56546	0.08244
OR2V2	-0.64827	0.07812	0.44958	0.047
C11orf63	-0.82981	0.09375	0.53174	0.00499
COX7A2L	-0.88839	0.05469	0.52409	0.03594
LIX1	-0.8274	0.0625	0.41204	0.02305
C9orf174	-1.23995	0.03125	0.71594	0.01195
MAPK14	-1.21113	0.03125	0.61718	0.00149
IDO1	-1.34244	0.01562	0.41761	0.05488
RAMP3	0.52548	0.07033	-1.01426	0.06366
NDNF	0.43955	0.08788	-0.7071	0.03983
DFNB31	0.6282	0.03015	-0.74608	0.04601
FEM1C	0.57947	0.07812	-0.58963	0.01008
IQCF6	0.5235	0.02661	-0.51587	0.00042
TOP2B	0.53156	0.073	-0.59619	0.07653
POTEM	0.43399	0.09375	-0.40957	0.02158
GMCL1	0.69676	0.0625	-0.54585	0.00257
RALGAPA2	0.79441	0.09375	-0.65342	0.071
CDH2	0.80081	0.0625	-0.47452	0.01647
TP53BP2	0.95885	0.0625	-0.57473	0.00074
TTF2	0.86936	0.03125	-0.43139	0.01178
KIRREL3	1.09696	0.07812	-0.64507	0.07968

G/V, GSKJ4 treated/vehicle treated.

Log2 values are averages of 24 and 72 h treatments.

Supplementary Table 3. Candidate genes for GSKJ4-caused expression alterations due to changes in K27me3 sequence association.